International Journal of Engineering Trends and Technology
ISSN: 2231 – 5381 /doi:10.14445/22315381/IJETT-V70I1P233
Volume 70 Issue 1, 283-290, January, 2022

Vibration-Based Condition Monitoring of a Tractor Radiator using Machine Vision System

Ganesan R[1], Dr.G.Sankaranarayanan[2], Dr.M.Pradeep Kumar[3], and Dr.V.K.Bupesh Raja[4]

[1]*Research scholar, Sathyabama Institute of Science and Technology, Chennai, India*
[2]*Supervisor, Sathyabama Institute of Science and Technology, Chennai, India*
[3]*Prof, Department of Mechanical Engineering CEGC, Anna University Chennai, India*
[4]*Prof, Mechanical Engineering, Sathyabama Institute of Science and Technology, Chennai, India*

[1]ganesanrcm@gmail.com, [2] gs2000narayanan@gmail.com, [3] pradeep@annauniv.edu

Abstract **-** *This research proposes a new intelligent fault detection and condition monitoring system of a cooling radiator of a tractor using machine vision systems. The proposed system consists of several different procedures, including image capturing, image pre-processing, and image processing. The proposed system, as a novel idea, uses a white paper sticker of known real-world dimensions marked with a colour dot or dots in it. The scaling factor is calculated by correlating the real-world sticker dimensions and camera image dimensions. The colour dot is considered as the target in the region of interest. The image was captured in a video format using a DSLR camera fitted with a macro lens. The macro lens offers image capturing at close-ups. The video images are processed through the template matching algorithm to calculate the displacement of the target point. The calculated displacement values are converted into acceleration values using mathematical relationships. The vibration is measured at the same point using a conventional accelerometer and Dewesoft interface. A good agreement of vibration measurement is recorded between the vibration measured by image vision systems and accelerometers. The mounting of the radiator can be repaired or replaced by referring to the manufacturer catalogue specifications.*

Keywords **-** *Condition monitoring, tractor radiator, machine vision, DSLR camera, macro lens*

I. INTRODUCTION

The radiator is a vital component of a compression ignition (CI) engine cooling system. The engine heat may reach up to 2700 °C under the maximum speed conditions owing to the internal gas temperature. The thermal expansion of the engine components, the change in viscosity index of lubricating oil, and knocking of the engine due to improper combustion are the outcomes of elevated engine temperature. The total thermal efficiency of the CI engine is affected by the performance of the radiator. Eddy current testing, radiography, vibration analysis, acoustic emission, and ultrasonic testing are traditional condition-based monitoring systems. Thermal imaging and machine vision systems are new condition-based monitoring methods. [1]

The tractor radiator must withstand the vibrations induced by the CI engine of the tractor and road. The radiator support brackets, rubber bushes, and mountings are subjected to fatigue stress and fatigue failure owing to the continuous fluctuating vibration amplitude. The crack induced by vibration will lead to leakage of coolant fluid, which affects the total performance of the tractor engine. The coolant pump and cooling fan are vital components of cooling systems. In addition, the cooling fan contributes to vibration to the engine and road vibrations. [2]

The coolant pump circulates the right amount of coolant through the radiator cooling circuit. The pump is also one of the sources of vibration due to the kinetic energy of the turbulent flow, velocity magnitude of the coolant fluid, and worn out in the bearings.[3]

The radiator of a tractor is subjected to vibrations from various sources. The need for fatigue analysis of the radiator parts is important to ensure better structural strength. The life of a spring can be predicted using nonlinear finite element analysis (FEA) software. The fatigue life can be calculated by fitting the S-N curve. The use of the Green-Lagrange strain method simplifies the calculations using a single function. The reliable operation of the tractor radiator is affected by vibration excitation by the engine, road, cooling fan, and cooling pump.[4-6]

The performance of the radiator, in general, affected by the following reasons

1. Leakage of the coolant due to crack-induced micro-cracks.
2. Leakage of the coolant due to corrosion-induced crack due to improper mixture coolant and additives.
3. Leakages due to perforations due to throwing of stone and debris up the radiator.
4. Leakage of the coolant due to excessive vibration in the plastic reservoir and aluminium core.

Condition-based monitoring (CBM) is one of the most significant and effective methods used to detect faults in a machine that helps maintain various machinery and equipment in a factory before repairs occur. Many scientific journals and case studies have shown that CBM provides significant advantages in saving considerable money and time in many industries.[7] Recent studies suggest that better maintenance is a way for a company to

make a profit. Science conferences and research papers have been campaigning in recent years that companies can maximize their profits through conditional monitoring. [8-10] Condition monitoring helps to know the inside information and brings it to the outside of a running machine. Vibration analysis and lubricant analysis are two important methods for condition monitoring. By observing the current state of a running machine, its future course can also be predicted. Condition monitoring helps determine the internal conditions of a running machine.

An engine is a set of rotating gears, shafts, etc., that can vibrate even when the machines are in good condition. These produce a certain frequency sequence as they rotate. These frequencies help detect the running nature of a machine. Therefore, various experiments were based on frequencies. Some vibrations do not have the same frequency continuously**;** for example, the vibration of an IC engine is not limited to its rotating parts. The strokes of the IC engine do not have a constant vibration because the engine performance depends on the speed and load of the engine**;** hence, there will be a change in frequency accordingly. Although it does not have a constant frequency, it is possible to analyze these frequency characteristics because they occur at regular intervals. Absolute vibration was calculated from the housing surface of the machine. Relative vibration is the frequency obtained from the parts separated by a thin lubricant fluid film. Diagnostic vibration information is calculated in the angular velocity variation influenced by parts such as shafts, gears, and rotor discs. Frequency calculations based on most condition monitoring were performed from the surface of the machine.

There are a few main ways to uncover the internal state of a running machine.

1. Vibration analysis: The machine will have a certain set of frequencies when it is in good condition. There will be a difference in the frequency setting when the machine is malfunctioning. We call this mechanical signature analysis. [11]
2. Lubricating-oil analysis: The metal particles present in the circulating lubricating oil inside the machine are the outcome of wear. The chemical change in the lubricating oil is the outcome of an increase in temperature beyond its limit owing to adverse working conditions of the running machine. Some of the oil tests are chip detectors, spectrograph oil analysis procedures, and ferrography.
3. Performance Analysis: The performance of the machine is calculated based on its output efficiency. If a certain level of efficiency is not available, it can be assumed that the machine has malfunctioned. The reason for this malfunction can be identified by the analysis.
4. Thermography is the most sophisticated computing tool used in recent times. This method is measured with the temperature changes that occur in the machine.

In many of the aforementioned methods, vibration-based condition monitoring is used in many industries.

Vibration can be calculated using software such as ANSYS. NASTRAN, however, its boundary conditions cannot be accurately stated. The vibration measured at different points is combined to analyze the overall performance of the machine or structure. Vibration calculations using contact sensors are mostly applied up to the present time. [12-14]

An acceleration sensor mounted on the surface of a machine can capture the frequency levels. The frequency calculation and vibration modelling methods should be considered separately. [15-18].Various studies have been conducted to calculate the vibration using different types of touch sensors. [19-20] New computational methods such as noncontact frequency detection methods are being used, but these new computational methods must be compared with the acceptable computational methods already in place [21,22].

The location where the non-contact vibration is intended to be calculated must be visible to capture the images. The shape of the machine may not be visible owing to its structural design, where the vibration must be calculated. Therefore, non-contact frequency measurement methods are subjected to limitations. The 3D vibrometer provided complete information about the vibration of the machine. However, the 1D vibrometer calculates the machine frequency directly through the hole, and vibration measurements were used to observe changes in the structures of mechanical and civil structures. The vibration calculation method can be divided into two types: non-contact and contact-type. Acceleration sensors are used for the calculation of contact-type vibrations. This will accurately calculate the vibrational frequencies. The new method of non-contact frequency calculation method should be confirmed by comparing it with the conventional method of calculation. In contact-type frequency calculation methods, the touch sensor adds some weight to the structure, which does not cause major changes when operated on a large structure in the vibration measurements. The additional weight of the sensor to the very small structure may cause changes in the calculated frequency. Another drawback of contact sensors is that they only calculate the frequency of where they are affixed. Therefore, it is not possible to calculate the absolute frequency of a structure. Contact sensors cannot be fitted where structures with high temperatures, rotating parts, or structures that are not easily accessible.

Laser Doppler vibrometry (LDV) contact-type frequency calculation method allows the calculation of the frequency at a specific location. The scanning laser vibrometer helps to calculate the vibrations occurring at different points in a structure. In the eddy current sensor, the frequency is measured by the electrical changes that occur in the gap between the sensor and the structure. This can only be implemented on an electrically conductive structure. The displacement at a point in the structure can be calculated by analyzing the video footage. Various

research papers suggest that the displacement in a structure can be accurately calculated using the digital image correlation technique. [23] three-dimensional displacement can be accurately calculated using two cameras. Stochastic speckle patterns must be made on the surface of the structure to calculate the deformation. [24] Digital photogrammetry is a non-contact, highly sensitive full-field measurement data that include photogrammetry, which includes optical measurements, computer vision, and digital image processing analysis. [25] Vibration can be calculated from the photo frames obtained by the camera using image processing techniques. [26, 27]

II. PROPOSED MACHINE VISION SYSTEM

Template matching is a basic component of machine vision practice for determining displacement. Many research articles claim that a template-matching algorithm is an excellent tool. With this template machine algorithm, two consecutive image images can be compared with the next position of the point in the image as a whole image template. [28, 29]

Assume an image I, with an offset of x=(x_a, x_b) and a template T of dimension r_T ×x c_T

. The error of the fit E(x) can be expressed,

$$Err(x) = \sum_{i==1}^{rT}\sum_{j=1}^{cT}\left(Tr_{i,j} - Ir_{xa+i,xb+j}\right)^2 = 0$$

Eqn.1

$$Err(x) = \sum_{k=1}^{rT}\sum_{l=1}^{cT}\left(Tr_{i,j}\right)^2 - 2\sum_{k=1}^{rT}\sum_{l=1}^{cT}\left(Tr_{i,j}Ir_{xa+i,xb+j}\right) + \sum_{k=1}^{rT}\sum_{l=1}^{cT}\left(Ir_{xa+i,xb+j}\right)^2 = 0$$

Eqn.2

$$\text{Corre}_T(x) = \sum_{k=1}^{rT}\sum_{l=1}^{cT}\left(Tr_{i,j}Ir_{xa+i,xb+j}\right) \qquad \text{Eqn.3}$$

A. Scaling Factor determination

When comparing images, these images also require a comparable real-world size. We call this the scaling factor. Before recording the video image, in this new method, the scaling factor arrived using a white paper sticker with a predetermined real-world dimension affixed to the object surface where the vibration is to be measured. The dots are marked with a colour on the sticker. The template was set by fixing the target at this point. The template algorithm compares two consecutive images and measures the variance of that point. [30-34]

B. Object tracking using Template matching through Up- sampled Cross-Correlation Algorithm

There are several types of template-matching algorithms. Up-sampled cross-correlation modified Taylor approximation Normalized cross-correlation are the important template algorithms.

$$\text{DFT(u,v)} = \sum_{x,y}\frac{f_{vf}(x,y)}{\sqrt{MN}}\exp\left[-i2\pi\left(\frac{ux}{M}+\frac{ux}{N}\right)\right]$$

Eqn.7

Equation (7) provides subpixel-level cross-correlation based on a time-efficient matrix multiplication discrete Fourier transform (MM-DFT) in a block around the initial peak of RFT to attain a subpixel resolution.

C. Calculation of acceleration for vibration measurement using finite element algorithm.

Measurements such as velocity and acceleration were calculated by a mathematical telephone with the help of a finite element algorithm to measure the displacement levels measured by the template matching algorithm. The aspiration measurements thus detected should be compared with the relational measurements calculated by the ration sensor in addition to the existing ones.

Acceleration

$$\text{axi} = \frac{\left(\begin{array}{l}2\times x(i+2) - x(i+1) - 2\times X(i) - \\ x(i-1) + 2\times X(i-2)\end{array}\right)}{\left(7\times\nabla t^2\right)}$$

Eqn.10

$$\text{ayi} = \frac{\left(\begin{array}{l}2\times y(i+2)y(i+1) - 2\times y(i) - \\ y(i-1) + 2\times y(i-2)\end{array}\right)}{\left(7\times\nabla t^2\right)}$$

Eqn.11

III. FIELD TESTS- EXPERIMENT SETUP

A. Experimental Model

Test specimen: Agricultural tractor, Model: TAFE 4410, Engine Power: 32.8 kW, Manual transmission, Wheelbase: 184 cm, Weight: 1999 kg

B. Camera

Canon Eos 5D Mark II DSLR with 21.1Megapixel, Sensor Size 36.0 x 24.00 mm, Pixel Dimensions 5616x3744, Pixel Size 6.41 μm, Diffraction- Limited Aperture f/10.3, Image sensor DIGIC 4, Movie Size 1920 × 1080, 640 × 480 at 30fps, Movie Length/Maximum duration 29m 59sec, Max file size4 GB, Came**ra** Lens: Macro Lens

C. Computer specifications

Toshiba Satellite-Laptop, Model: C640-I401A, processor: Intel Core i3-370M, RAM: 2GB, internal storage: 320 GB, screen size: 14.0 inches.

D. Vibration Measurement system

USB powered data acquisition: SIRIUS® MINI, Software: Dewesoft NVH analysis software, Number of

axes: 3, Accelerometer Sensors: 13TI-50G-1, Type: IEPE, Sensitivity: 100mV/g, Weight: 10 g, Frequency range: 2 to 5000 Hz ± 10%, Dimensions: 15.0 × 15 × 15 mm, Temperature Range: -51 degrees to +85 °

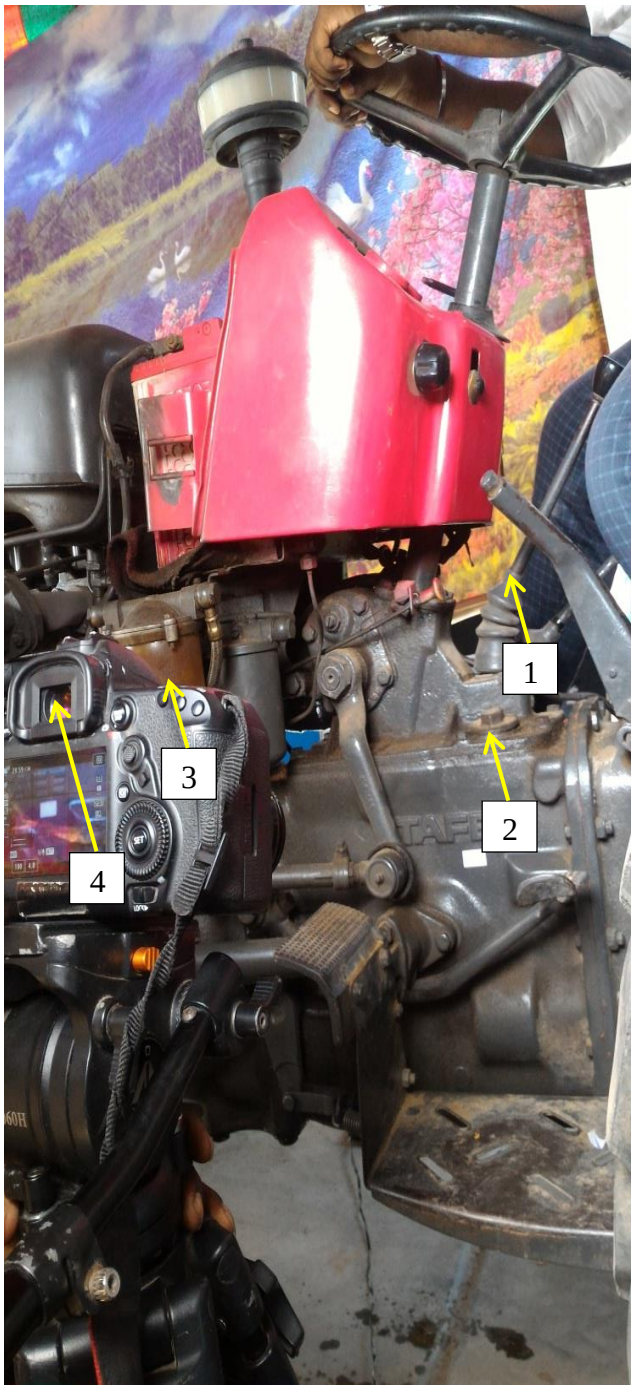

Figure1 Experiment setup –close view

1. Agricultural Tractor
2. Paper sticker with real-world dimensions
3. DSLR Camera
4. Camera screen showing the image of the scene.

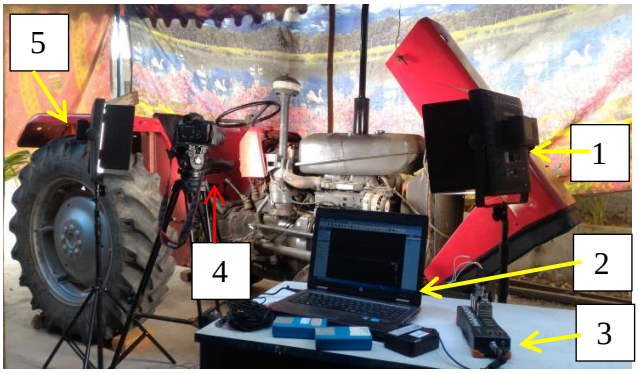

Figure 2: Experimental setup- Overall view

1. LED light source 2. Computer system
3. Acceleration sensor interface 4. DSLR Camera
5. Agricultural Tractor

Figures 1 and 2 show the experimental setup, an agricultural tractor, an LED light source with variable current switch to change the intensity of light, a DSLR camera, a computer system, and an interface for the accelerometer sensor are shown in the figure.

IV. EXPERIMENTAL METHOD

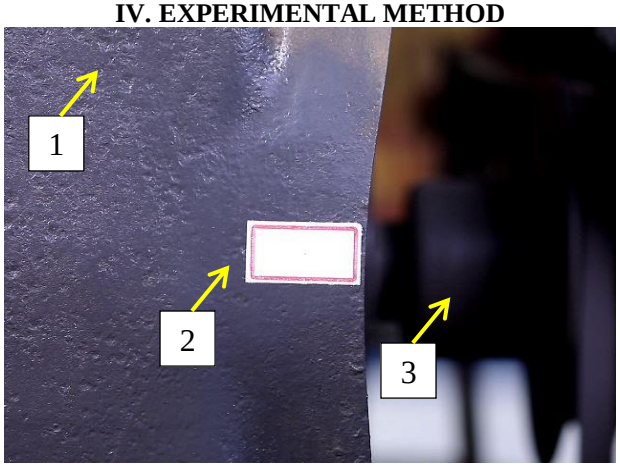

Figure3. Radiator body

1. Radiator body
2. Paper sticker affixed on the radiator body
3. Radiator fan

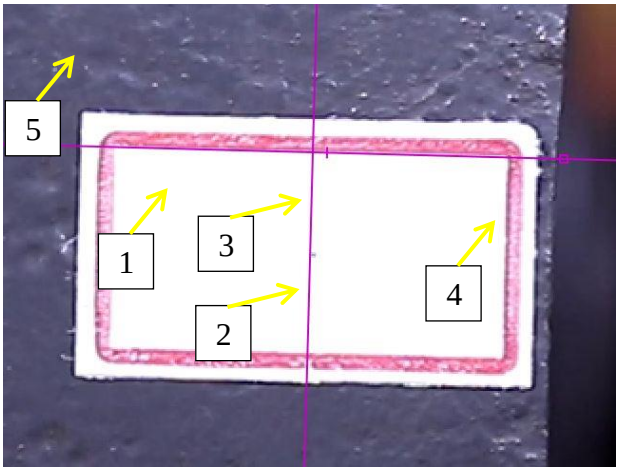

Figure4. Reference paper sticker on the radiator body

1. x-axis 2. Target point 3. y-axis
4. Real-world reference line
5. Radiator body

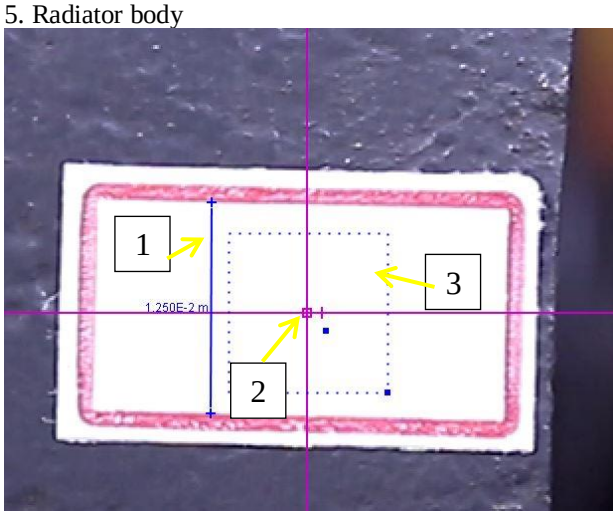

Figure5. Paper sticker details

1. Real-world dimensions line
2. x-y axes set to (0, 0) at the target point
3. Region of interest (ROI)

Canon DSLR EOS50 Mark II can produce videos of 640 × 480 and 1920 × 1080 pixels at 100fps and 30fps, respectively. In a 640 × 480 pixel video frame, the left bottom corner measures (0.0, 0.0) and the right top corner measures (640 × 480). A paper sticker with known was affixed to the radiator body, where the video was captured for vibration analysis. The sticker of the real-world dimension is correlated with the image dimensions in pixels and using a suitable conversion factor, and the image dimensions were fixed to the real-world dimensions. [35-38]

Figures 3, 4, and 5 show the practical arrangement of paper stickers with real-world dimensions. The length and height of the sticker were used to specify real-world dimensions. The colour dot in the sticker can be a target point; alternatively, any point in the sticker may be taken as the target point. At least one key-frame is required to perform the programmable search in a template matching the displacement. The up-sampled cross-correlation algorithm calculates the displacement with sub-pixel accuracy. The template is matched when the sum of squares is the maximum between match pixel and template pixels of RGB contrast. [39 -41]

V. RESULTS

Figure6 to Figure14 the legends coloured in red show the acceleration value derived from the image vision process mathematical algorithm. The legend in blue is the acceleration values measured from the conventional acceleration sensors and Dewesoft interfacing software. The graph trend shows a good agreement between the two measurement techniques.

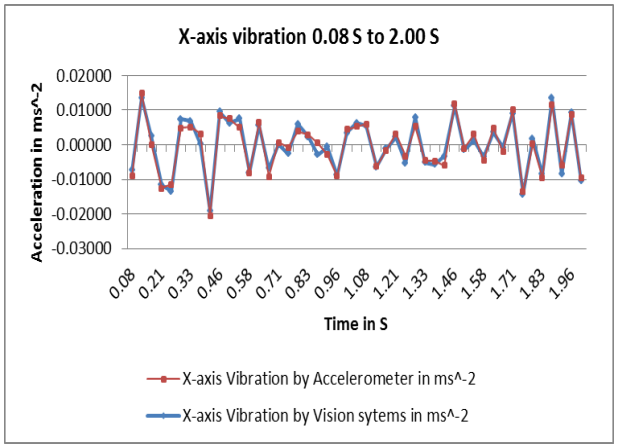

Figure6 Vibration comparisons for two seconds (0.08 to 1.96 Sec)

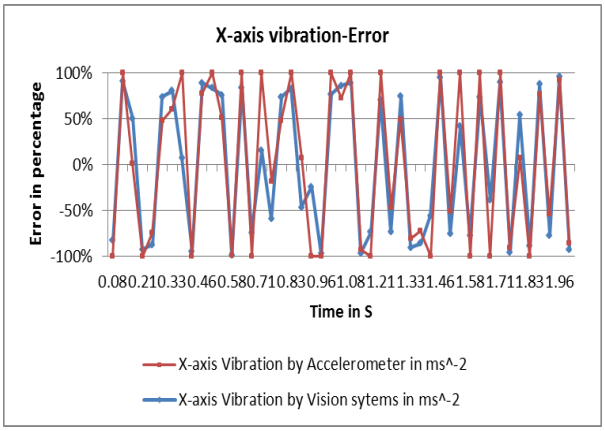

Figure7 Vibration error comparisons for two seconds (0.08 to 1.96 Sec)

Figure6 show the vibration trends for the period of 0.08 seconds to 1.96 seconds, and the graph was plotted between time and x-axis acceleration.
Figure7 show the vibration error for the period of 0.08 seconds to 1.96 seconds, and the graph was plotted between time and x-axis acceleration.

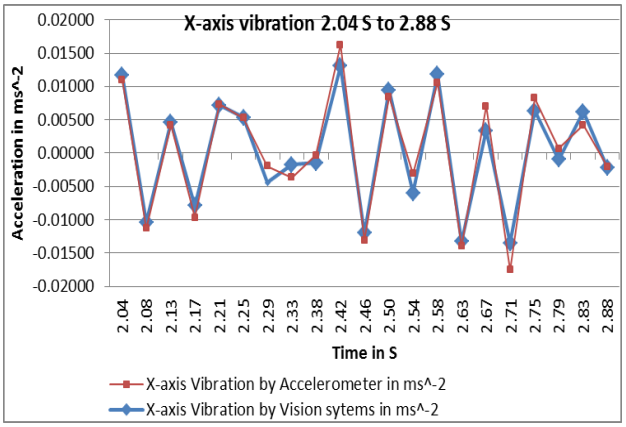

Figure8 Vibration comparisons for one second (2.04 to 2.88 Sec)

Figure8 show the vibration trends for the period of 2.04 seconds to 2.88 seconds, and the graph was plotted between time and x-axis acceleration.

Figure9 show the vibration error for the period of 2.04 seconds to 2.88 seconds, and the graph was plotted between time and x-axis acceleration.

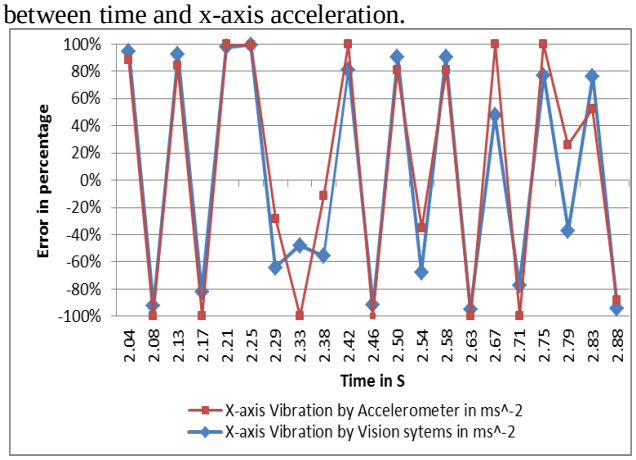

Figure9 Vibration error comparisons for two seconds (2.04 to 2.88 Sec)

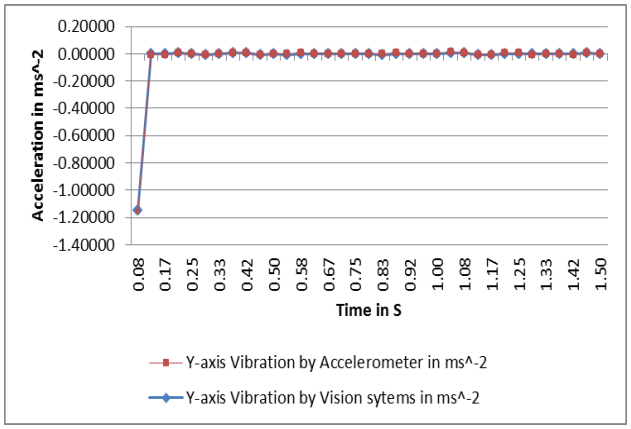

Figure10 Vibration comparisons for 1.5 seconds (0.08 to 1.50 Sec)

Figure10 show the vibration trends for the period of 0.08seconds to 1.50 seconds, and the graph was plotted between time and y-axis acceleration. The vibration measured by machine vision shows a significant error at 0.08sec because of shake of camera shaking during the initial manual operation.

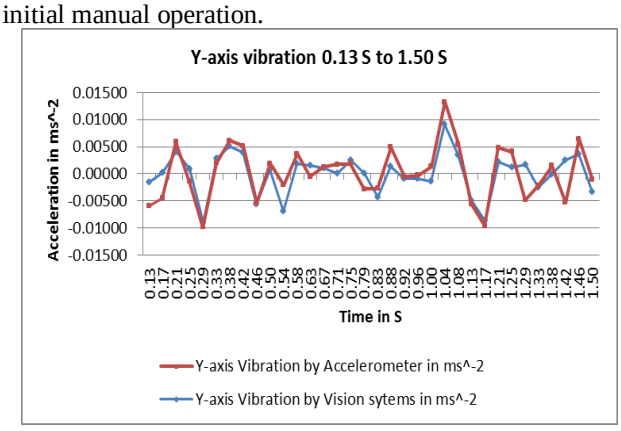

Figure11 Vibration comparisons for 1.5 seconds (0.08 to 1.50 Sec)

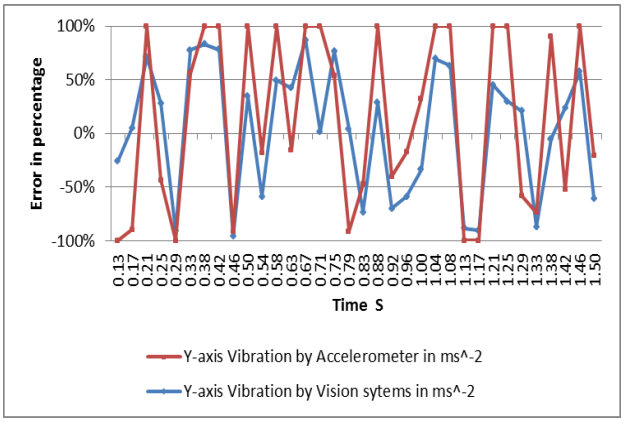

Figure12 Vibration error comparisons for 1.5 seconds (0.13to 1.50 Sec)

Figure11 shows the vibration trends for the period of 0.13 seconds to 1.50 seconds, and the graph was plotted between time and y-axis acceleration.

Figure12 show the vibration error for the period of 0.13 seconds to 1.50 seconds, and the graph was plotted between time and y-axis acceleration.

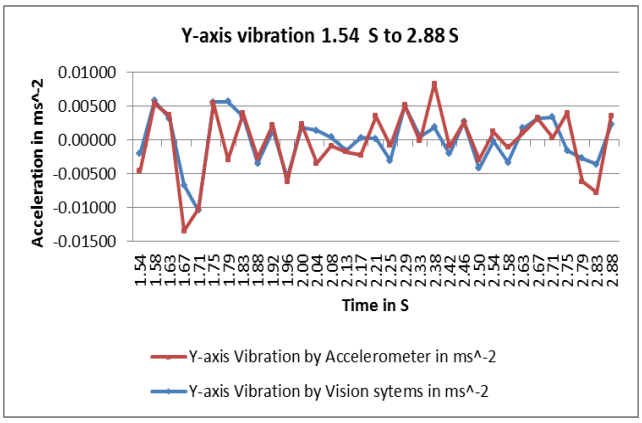

Figure13 Vibration comparisons for 1.5 seconds (1.54 to 2.88 Sec)

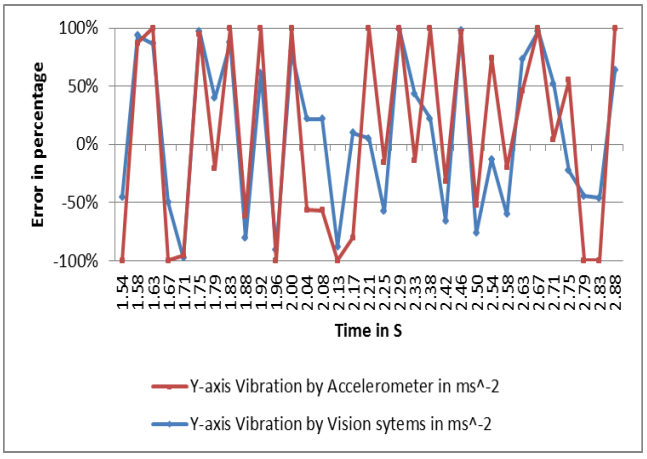

Figure14 Vibration error comparisons for 1.5 seconds (1.54 to 2.88 Sec)

Figure13 show the vibration trends for the period of 1.5 seconds to 2.88 seconds, and the graph was plotted between time and y-axis acceleration.

Figure14 show the vibration error for the period of 1.5 seconds to 2.88 seconds, and the graph was plotted between time and y-axis acceleration.

VI. DISCUSSION

References [42, 43, 44, 45, and 46] verified the algorithm used in the vision sensor and the proposed vision system. References [47, 48] confirmed the results and the percentage of error. The lower the displacement values, the higher the percentage of error; the percentage of error is comparable to the higher value of displacements. The minimum size of the proposed machine sight system is 0.01 mm displacement.

References [49, 50] suggest the suitable anti-vibration mounting which keeps the radiator working within the vibration limits to avoid vibration-related fatigue failures of radiator components.

VII. CONCLUSIONS

The following conclusions have been made,

a) The proposed system is best suited for vibration measurement of stationary machines with low-frequency limits. The use of a macro lens helps capture very close image frames. Close-up images assign real-world dimensions to a white sticker known to achieve an accuracy of 0.01 mm and help mark the smallest target in the area of interest.

b). The percentage of error was recorded at very low vibration values ranging from zero to 5% to 50%, whereas the essential limit for vibration analysis was recorded at 5% to 10% error. However, the map trends follow the same path for all sets of data.

c) The proposed probe avoids the difficulty of camera calibration. A white sticker of known real-world dimensions is used to raise the scaling factor because the dimension of the image is adjusted with an accuracy of less than one mm with a real-world dimension. The white sticker reduces noise in the background image. Image processing is performed without pre-processing the images to calculate sub-pixel-level displacements to save time and memory.

d). Different intensities of light did not differ significantly in the measurement of the vibration levels. As a template search for calculating displacement accounts only for changes between the target point intensity and background intensity. The change in light intensity caused the same amount of change throughout the image.

e) The amount of vibration measured by the machine sight system using the mathematical method is less than the values of conventional accelerometer measurements, which may be due to the sensitivity of the accelerometer sensor. Image processing is performed by targeting the smallest point in the area of interest in an image frame. Further research is required to determine the exact cause of this error.

f). The measurement data have comparable precision graphing trends that can be used as a non-contact vibration-measuring instrument in an automated level monitoring system.

g). Further vibration study is needed to be done at each mounting to maintain or replace the mouuntigs.

Data availability statement

All data supporting the findings of this study are included within the article (and any supplementary files).

Conflict of interest

The authors declare no competing financial interests or personal relationships that could influence the work reported in this paper.

Funding statement

The funders had no role in the study design, data collection and analysis, decision to publish, or preparation of the manuscript.

REFERENCES

[1] AminTaheri-Garavand et al., An intelligent approach for cooling radiator fault diagnosis based on infrared thermal image processing technique, Applied Thermal Engineering 87 (2015) 434-443 http,//dx.doi.org/10.1016/j.applthermaleng.2015.05.038,1359-4311/

[2] N F D Razak et al., Noise and vibration analysis for automotive radiator cooling fan, IOP Conf. Series, Materials Science and Engineering 257 (2017) 012083i,10.1088/1757-899X/257/1/012083

[3] Dr S B Prakash, CFD Analysis of a Radiator Pump to Investigate the Cause and to Eliminate the Unwanted Vibrations, International Journal of Research Studies in Science, Engineering and Technology, 1(5) (2014) 52-59

[4] Ismael, T. and Sheng, B.Y., Radiator Vibration Fatigue Analysis. Journal of Electronics Cooling and Thermal Control, 7 (2017) 8-21. https,//doi.org/10.4236/jectc.2017.71002

[5] Li, Q., Zhao, J.-C. and Zhao, B., [3] Li, Q., Zhao, J.-C. and Zhao, B., Fatigue Life Prediction of a Rubber Mount Based on Test of Material Properties and Finite Element Analysis. Engineering Failure Analysis, 16 (2009) 2304-2310. https,//doi.org/10.1016/j.engfailanal.2009.03.008

[6] Luo, R.K. and Wu, W.X., Fatigue Failure Analysis of Anti-Vibration Rubber Spring. Engineering Failure Analysis, 13 (2006) 110-116. https,//doi.org/10.1016/j.engfailanal.2004.10.012

[7] Rao, B.K.N., Advances in diagnostic and prognostic strategies and technologies for failure-free maintenance of industrial assets. Comadem, San Sebastian, Spain, (2009) 9–11.

[8] Al-Najjar, B. and Alsyouf, I., Enhancing a company's profitability and competitiveness using integrated vibration-based maintenance, a case study. Journal of European Operation Research, 157 (2004) 643–657.

[9] Al-Najjar, B., A maintenance model for identification, quantification and elimination of losses in companies profitability, an application example. Comadem, San Sebastian, Spain, (2009) 9–11.

[10] Vlok, P.J., Coetzee, J.L., Banjevic, D. et al., Optimal component replacement decisions using vibration monitoring and the PHM. Journal of the OR Society, 53 (2002) 193–202.

[11] Braun, S. (ed.) (1986) Mechanical Signature Analysis, Academic Press, London.

[12] D. Biermann, A. Zabel, T. Brüggemann, A. Barthelmey, A comparison of low-cost structure-borne sound measurement and acceleration measurement for detection of workpiece vibrations in 5-axis simultaneous machining. Procedia CIRP, 12 (2013) 91-96.

[13] M. Watanabe, H. Iki, K. Sakamoto, Y. Uriu, Y. Kado, Analysis of turbine generator shaft torsional vibration caused by self-commutated converters. IEEJ Transactions on Power and Energy. 134 (11) (2013) 900-907.

[14] Alok Sinha. Reduced-Order Model of a Bladed Rotor With Geometric Mistuning. J. Turbo, vol. 131 (3) (2009), 199-207.
[15] J. Zhai, H. Zhang, Q. Han, D. Wang, Y. Liu, Modeling and experiments of rotor system with oil-block inside its drum cavity. Journal of Vibroengineering, 150 (4) (2013) 1972-1982.
[16] J. Cheng, Y, Wang, C.J. Cui, Finite element dynamic analysis of the shafting of transmission-laser-scanning-emitter. Advanced Materials Research, 697 (2013) 190-193.
[17] S.A.A. Hosseini, S.E. Khadem, Free vibrations analysis of a rotating shaft with nonlinearities in curvature and inertia. Mechanism and Machine Theory 44(1) (2009) 272-288.
[18] S. Braut, R. Žigulić, M. Butković, Numerical and experimental analysis of a shaft bow influence on a rotor to stator contact dynamics. Strojniski Vestnik/Journal of Mechanical Engineering. 54 (10) (2008) 693-706.
[19] X. Qian, G. Lin, X. Du, Vibration measurement and data analysis of a spinning shaft using a camera-based motion analysis system. Applied Mechanics and Materials, 29-32 (2010) 203-208.
[20] Adolfo Senatore. Measuring the natural frequencies of the centrifugally tensioned beam with a laser doppler vibrometer. Measurement Techniques, 39 (2006) 628-633.
[21] Yu, M., Guo, J., Lee, K.-M. Strain field sensing and reconstruction for a thin-wall plate. IEEE/ASME International Conference on Advanced Intelligent Mechatronics, AIM. 2016 – September, 7576864 (2016) 788-793.
[22] Goyal, D., Pabla, B.S. Development of non-contact structural health monitoring system for machine tools. Journal of Applied Research and Technology, 14 (4) (2016) 245-258.
[23] T. Chu, W. Ranson, M. Sutton, Applications of digital-image-correlation techniques to experimental mechanics, Exp. Mech. 25 (1985) 232–244.
[24] M.N. Helfrick, C. Niezrecki, P. Avitabile, T. Schmidt, 3D digital image correlation methods for full-field vibration measurement, Mech. Syst. Signal Process. 25 (2011) 917–927.
[25] Y.-Z. Song, C.R. Bowen, H.A. Kim, A. Nassehi, J. Padget, N. Gathercole, A. Dent, Non-invasive damage detection in beams using marker extraction and wavelets, Mech. Syst. Signal Process. 49 (2014) 13–23.
[26] James R. Parker, Algorithms for Image Processing and Computer Vision, John Wiley &Sons, New York, 1997
[27] R. C. Gonzalez and R. E. Woods, Digital Image Processing, Addison Wesley, 1992.
[28] S. Geethapriya, K. Devaki, V. Murali Bhaskaran, Multiple Object Detection in Images using Template Matching, International Journal of Innovative Technology and Exploring Engineering (IJITEE) ISSN, 2278-3075, 9(1) (2019), DOI, 10.35940/ijitee.A5187.119119
[29] D.H. Diamond, P.S. Heyns, A.J. Oberholster, Accuracy evaluation of sub-pixel structural vibration measurements through optical flow analysis of a video sequence, Measurement, http,//dx.doi.org/10.1016/j.measurement.2016.10.0210263-2241/
[30] Hijazi, A.; Friedl, A., Kähler, C.J. Influence of camera's optical axis non-perpendicularity on the measurement accuracy of two-dimensional digital image correlation. Jordan J. Mech. Ind. Eng. 5 (2011) 373–382.
[31] Dongming Feng, Maria Q. Feng, Ekin Ozer and Yoshio Fukuda, A Vision-Based Sensor for Noncontact Structural Displacement Measurement, doi,10.3390/s150716557
[32] Sładek, J., Ostrowska, K.; Kohut, P.; Holak, K., Gąska, A.; Uhl, T. Development of a vision based deflection measurement system and its accuracy assessment. Measurement, 46 (2013) 1237–1249.
[33] Zhang, Z. A flexible new technique for camera calibration. IEEE Trans. Pattern Anal. Mach. Intell. 22 (2000) 1330–1334.
[34] Dworakowski, Z.; Kohut, P.; Gallina, A.; Holak, K.; Uhl, T. Vision-Based algorithms for damage detection and localization in structural health monitoring. Struct. Control Health Monit., 23(1) (2015) 35-50, doi,10.1002/stc.1755.
[35] Hijazi, A., Friedl, A., Kähler, C.J. Influence of camera's optical axis non-perpendicularity on the measurement accuracy of two-dimensional digital image correlation. Jordan J. Mech. Ind. Eng., 5, (2011) 373–382.
[36] Dongming Feng, Maria Q. Feng, Ekin Ozer and Yoshio Fukuda, A Vision-Based Sensor for Noncontact Structural Displacement Measurement, doi,10.3390/s150716557
[37] Sładek, J., Ostrowska, K.; Kohut, P.; Holak, K.; Gąska, A., Uhl, T. Development of a vision based deflection measurement system and its accuracy assessment. Measurement 46 (2013) 1237–1249.
[38] Dworakowski, Z.; Kohut, P.; Gallina, A.; Holak, K.; Uhl, T. Vision-Based algorithms for damage detection and localization in structural health monitoring. Struct. Control Health Monit., 23(1) (2015) 35-50, doi,10.1002/stc.1755.
[39] Douglas Brown Innovative Uses of Video Analysis, The Physics Teacher 47 (2009) 145 https,//doi.org/10.1119/1.3081296.
[40] Chris Eberl, Robert Thompson, Daniel Gianola, Sven Bundschuh, @ Karlsruhe Institute of Technology, Germany, Group of Chris Eberl,@ Johns Hopkins University, USA, Group of Kevin J. Hemker, Digital Image Correlation and Tracking with Matlab
[41] https,//in.mathworks.com/
[42] Bing you Liu, Dashan Zhang, Jie Guo, Chang'an Zhu, Vision-based displacement measurement sensor using modified Taylor approximation approach, Opt. Eng. 55(11) (2016) 114103, doi, 10.1117/1.OE.55.11.114103.
[43] Dongming Feng, Maria Q. Feng, Ekin Ozer and Yoshio Fukuda, A Vision-Based Sensor for Noncontact Structural Displacement Measurement, doi,10.3390/s150716557
[44] Dashan Zhang, Jie Guo, Xiujun Lei and Changan Zhu, A High-Speed Vision-Based Sensor for Dynamic Vibration Analysis Using Fast MotionExtraction Algorithms, Sensors 16 (2016) 572; doi,10.3390/s16040572.
[45] Junhwa Lee, Kyoung-Chan Lee, Soojin Cho, and Sung-Han Sim, Computer Vision-Based Structural Displacement Measurement Robust to Light-Induced Image Degradation for In-Service Bridges, Sensors (2017), 17, 2317; doi,10.3390/s17102317
[46] Jaka Javh, Janko Slavic, Miha Boltezar Measuring full-eld displacement spectral components using photographs taken with a DSLR camera via an analogue Fourier integral Mechanical Systems and Signal Processing, 100 (2018) 17-27, DOI, 10.1016/j.ymssp.2017.07.024
[47] Ming Yang, Chenguang Cai, Ying Wang1, Haijiang Zhu1, Zhihua Liu, A Novel Low-Frequency Vibration Measurement Method Based on Single Camera, Ming Yang et al. ,J. Phys., Conf. Ser. 1065 (2018), doi,10.1088/1742-6596/1065/22/222016222016,
[48] Wu et al., Cost-effective, vision-based multi-target tracking approach for structural health monitoring, Meas. Sci. Technol. 32 (2021) 125116 (18pp) https,//doi.org/10.1088/1361-6501/ac2551
[49] KURASHIKI KAKO CO., LTD. Industrial Products Division-Industrial Vibration Solutions https,//www.kuraka.co.jp/en/download/pdf/industrial_sangyototal_en.pdf
[50] A.M. Noor Azammi et al. Conceptual design of automobile engine rubber mounting composite using TRIZ-Morphological chart-analytic network process technique, Defence Technology 14 (2018) 268e277